Available online at www.sciencedirect.com
SCIENCE DIRECT®
International Journal of Thermal Sciences 43 (2004) 1075–1090
International Journal of Thermal Sciences
www.elsevier.com/locate/ijts

Adaptive neuro-fuzzy modeling of transient heat transfer in circular duct air flow

Abdulsamet Hasiloglu [a], Mehmet Yilmaz [b,*], Omer Comakli [b], İsmail Ekmekci [c]

[a] *Department of Electronics and Telecommunications Engineering, Engineering Faculty, Ataturk University, Erzurum, Turkey*
[b] *Department of Mechanical Engineering, Engineering Faculty, Ataturk University, Erzurum, Turkey*
[c] *Department of Mechanical Engineering, Engineering Faculty, Sakarya University, Sakarya, Turkey*

Received 30 September 2002; received in revised form 30 June 2003; accepted 20 January 2004

Available online 28 May 2004

Abstract

The aim of this study is to demonstrate the usefulness of an adaptive neuro-fuzzy inference system (ANFIS) for the prediction of transient heat transfer. An ANFIS has been applied for the transient heat transfer in thermally and simultaneously developing circular duct flow, subjected to a sinusoidally varying inlet temperature. The experiments covered Reynolds numbers in the $2528 \leqslant Re \leqslant 4265$ range and inlet heat input in the $0.01 \leqslant \beta \leqslant 0.96$ Hz frequency range. The accuracy of predictions and the adaptability of the ANFIS were examined, and good predictions were achieved for the temperature amplitudes of the transient heat transfer in thermally and simultaneously developing circular duct flow. The results show that the neuro-fuzzy can be used for modeling transient heat transfer in ducts. The results obtained with the ANFIS are also compared to those of a multiple linear regression and a neural network with a multi-layered feed-forward back-propagation algorithm.

Keywords: Transient heat transfer; Duct; Forced convection; Neural network; Fuzzy; Neuro-fuzzy

1. Introduction

Transient convective heat transfer in tubes and ducts is very important in connection with the control of modern high performance heat transfer devices, and has been widely studied [1–13]. Problems arising from start-ups, shut-downs, power surges and pump failures etc., during normal operating conditions or time-varying inlet temperature and flow rates can induce the transient behavior in thermal equipment. Thermal transients in ducts may also arise because of time dependent wall heat flux, as in the case of solar collector; wall temperature, or internal heat generation, as in the flow channels of nuclear reactors. In these systems, ducts are generally the basic parts that may be exposed to many planned or unplanned transients, and an accurate prediction of the thermal response for such systems during unsteady periods is very important; otherwise, the behavior of thermal system's response with-time can produce undesirable effects, leading to mechanical failure [11]. For these reasons, transient convective heat transfer in ducts has been extensively investigated by experimental, analytical and various numerical methods.

Although there are various experimental investigations on the transient heat transfer in ducts, the cost of experimental studies is very high. Numerical and different approximation methods are alternative methods for further analysis because their cost is cheaper than others [14]. Brown et al. [6], Kawamura [7], Travelho and Santos [8], Chen et al. [9], Kakaç and Yener [10] etc. are among the investigators who analyzed the transient heat transfer in ducts numerically.

Artificial neural networks (ANNs) have become popular because of their high computational rates, robustness and ability to learn, and they have been used in diverse applications in power systems, manufacturing, optimization, medicine, signal processing, control, robotics, and social/psychological sciences [15,16]. Fuzzy logic is a problem-solving technique that derives its power from its

* Corresponding author. Fax: +90 442 2360957.
E-mail addresses: asamet@atauni.edu.tr (A. Hasiloglu), yilmazm@mailcity.com (M. Yilmaz), ocomakli@atauni.edu.tr (O. Comakli), ekmekci@sakarya.edu.tr (İ. Ekmekci).

1290-0729/$ – see front matter
doi:10.1016/j.ijthermalsci.2004.01.010

Nomenclature

D	diameter of orifice plate	m
D_p	duct diameter of fan redevelopment	m
D_t	diameter of test section	m
f	logistic sigmoid activation function	
h	hidden layer	
O	output	
OL	output layer	
p	design parameter (consequent parameter)	
q	design parameter (consequent parameter)	
r	design parameter (consequent parameter)	
Re_p	Reynolds number in the fan redevelopment section	
Re_t	Reynolds number in the test section	
t	time	
T	temperature	°C
w	wiring strength of a rule	
W	weights	
X	axial distance	m
X	input	
Y	target activation of the output layer	

Greek symbols

α	dimensionless decay index	
α	learning rate	
β	frequency of inlet periodic heat input	Hz
δ	error for output neuron	
θ	dimensionless amplitude, $\Delta T/\Delta T_0$	
θ	threshold between the input and hidden layers	
ε_1	expansion factor	
η	momentum factor	
ρ	density	$\mathrm{kg\cdot m^{-3}}$
ΔP	orifice plate pressure drop	Pa
ΔT	centerline temperature amplitude	°C
ΔT_0	temperature amplitude at the center of the inlet	°C
μ	dynamic viscosity	$\mathrm{N\cdot s\cdot m^{-2}}$
φ	amplitude variation	

Subscripts

i	input
max	maximum
min	minimum
o	output
p	value related to the redevelopment section
t	value related to the test section
amp	amplitude

ability to draw conclusions and generate responses based on vague, ambiguous, incomplete and imprecise information. To simulate this process of human reasoning it applies the mathematical theory of fuzzy sets first defined by Professor Lotfi Zadeh, in 1965 [17]. ANFIS (Adaptive Neuro-Fuzzy Inference Systems), developed in the early 90s by Jang [18], incorporates the concept of fuzzy logic into the neural networks to facilitate learning and adaptation.

ANNs have been used by various investigators for modeling and predictions in the field of energy-engineering systems. Kalogirou [15] presents various applications of the ANNs in the field of energy-engineering systems in a thematic way: solar steam generator, solar water heating systems, heating, ventilating and air conditioning (HVAC) systems, solar radiation and wind speed predictions, power generation systems, forecasting and prediction, refrigeration etc. The number of investigations that evaluate convective heat transfer using artificial intelligence techniques is limited. Thibault and Grandjean [19] presented a neural network methodology for heat transfer data analysis. Three different examples were solved, using a three-layer feedforward neural network. It was shown that neural networks could be used to adequately correlate heat transfer data. Jambunathan et al. [20] evaluated convective heat transfer coefficients using neural networks. The backpropogation algorithm was used to predict heat transfer coefficients from a given set of experimentally obtained conditions. Diaz et al. [21] proposed a methodology for training and prediction of the dynamic behavior of thermal systems with heat exchangers. The artificial neural network technique was extended to the simulation of the time-dependent behavior of a heat exchanger and used to control the temperature of air passing over it. A neural network approach was used to a nonlinear identification and control of a heat exchanger by Bittati and Piroddi [22]. Scalabrin and Piazza [23] presented the modeling of forced convection heat transfer for carbon dioxide flowing inside a heated tube at supercritical conditions. Four different correlation architectures were considered for the neural network function, alternatively based on dimensionless groups and on directly accessible physical quantities as independent variables.

Artificial intelligence (AI) techniques can provide a fundamentally different approach to transient heat transfer in ducts than numerical solution methods. Artificial intelligence in the form of expert systems and/or neural networks can provide an affordable means of capturing the transient heat transfer data and knowledge in a documented form available for all. On the other hand, review of literature on artificial intelligence systems in the area of transient heat transfer reveals that only a limited number of studies have been reported [14]. Ekmekçi et al. [14] presents the results of an investigation on forced convection in a duct with artificial neural network. A multilayered feed-forward back-propagation neural network algorithm was used to predict the temperature distribution in a duct with a periodically varying inlet temperature in hydrodynamically developed

and thermally developing unsteady laminar convection. To the author's knowledge, there is no study on the application of neuro-fuzzy systems to transient heat transfer in a duct. The purpose of this study is to apply an adaptive neuro-fuzzy intelligence system to transient heat transfer. The experimental results of transient forced convection with thermally developing and simultaneously developing airflow within a circular duct are used. A traditional data-mining and a neural network technique are also used for comparison purposes, and the results were compared to those of the ANFIS.

2. Neural networks

Algorithms for analytic computer codes in engineering systems are usually complicated, involving the solution of complex differential equations. These programs usually require large computer power and need a considerable amount of time to give accurate predictions. Instead of complex rules and mathematical routines, artificial neural-networks are able to learn the key information patterns within a multi-dimensional information domain. In addition, they are fault tolerant in the sense that they are able to handle noisy and incomplete data, are able to deal with non-linear problems, and once trained can perform predictions and generalizations at high speed [15].

A neural network is a computational structure, consisting of a number of highly interconnected processing elements (or nodes) that produces a dynamic response to external input or stimuli. Neural networks were originally developed as approximations of the capabilities exhibited by biological neural systems, and they are based on a connectionist structure and mathematical functions that imitate the architecture and functions of the human brain. An artificial neural network consists of interconnected artificial neurons, interacting with one another in a concerted manner. Much of the interest in neural networks arises from their ability to learn to recognize patterns in large data sets. This is accomplished by presenting the neural network with a series of examples of the conditions that the network is being trained to represent. The neural network then learns the governing relationships in the data set by adjusting the weights between its nodes. In essence, a neural network can be viewed as a function that maps input vectors to output vectors [16,24].

In this study, a multi-layered feed-forward back-propagation algorithm is used. Input–output pairs are presented to the network, and weights are adjusted to minimize the error between the network output and the actual value. Fig. 1 shows the back-propagation model, which has three layers of neurons: an input layer, a hidden layer, and an output layer [25]. The back-propagation training algorithm is an iterative gradient algorithm, designed to minimize the mean square error between the predicted output and the desired output. The flow chart of the back-propagation learning algorithm is illustrated in Fig. 2. The algorithm of training a back-propagation network is summarized as follows [14]:

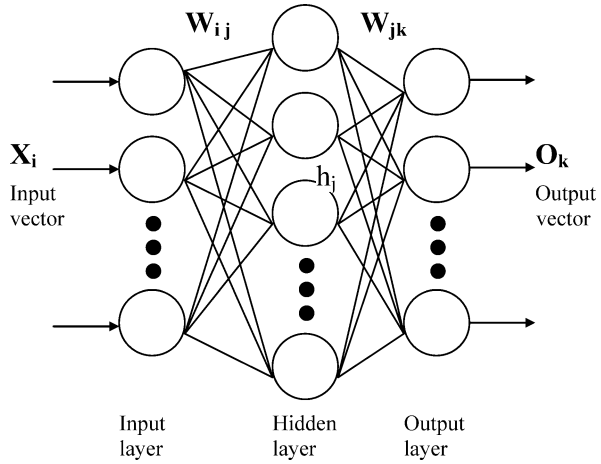

Fig. 1. A three-layer feed-forward neural network used in this study.

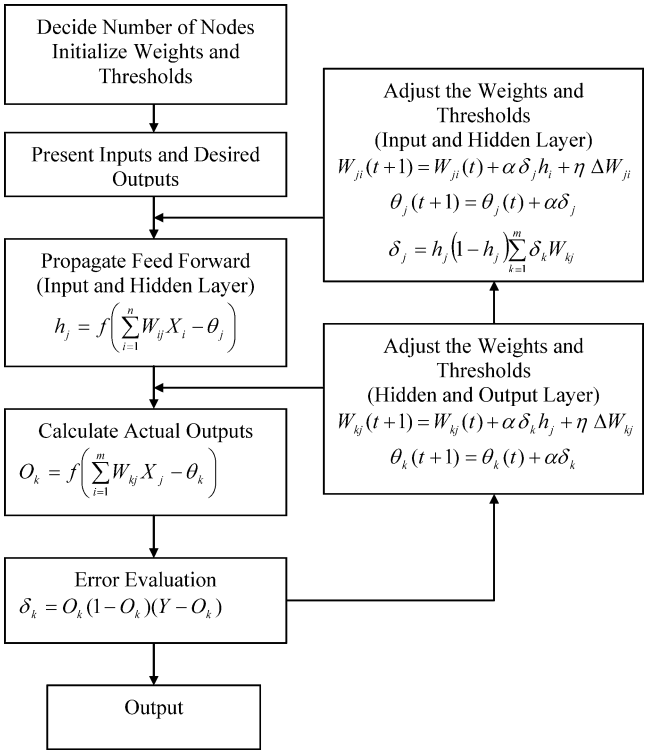

Fig. 2. Flow chart of the back-propagation learning algorithm.

(1) Initialize weights and threshold values: set all weights and threshold to small random values.
(2) Present input and desired output: present a continuous valued input vector $X_1, X_2, \ldots, X_n$, and specify the desired outputs $O_1, O_2, \ldots, O_n$. Usually the training sets are normalized to values between -0.9 and 0.9 during processing.
(3) Compute the output of each node in the hidden layer:

$$h_i = f\left(\sum_{i=1}^{n} W_{ij} X_i - \theta_j\right) \tag{1}$$

where h_j is the vector of hidden-layer neurons, i is the input-layer neurons, W_{ij} are the weights between the

input and hidden layers, and θ_j is the threshold between the input and hidden layers.

(4) Compute the output of each node in the output layer:

$$O_k = f\left(\sum_{i=1}^{m} W_{kj} X_j - \theta_k\right) \tag{2}$$

where k represent the output layer, W_{kj} are the weights connecting the hidden and output layers, θ_k is the threshold connecting the hidden and output layers, and $f(x)$ is a logistic sigmoid activation function:

$$f(x) = \frac{1}{1+e^{-x}} \tag{3}$$

(5) Compute the output layer error between the target and the observed output:

$$\delta_k = O_k(1-O_k)(Y-O_k) \tag{4}$$

where δ_k is the vector of errors for each output neuron and Y is the target activation of output layer.

(6) Compute the hidden layer error:

$$\delta_j = h_j(1-h_j)\sum_{k=1}^{m} \delta_k W_{kj} \tag{5}$$

where δ_j is the vector of errors for each hidden layer neuron.

(7) Adjust the weights and thresholds in the output layer:

$$W_{kj}(t+1) = W_{kj}(t) + \alpha\delta_k h_j + \eta\big(W_{kj}(t) - W_{kj}(t-1)\big) \tag{6}$$

$$\theta_k(t+1) = \theta_k(t) + \alpha\delta_k \tag{7}$$

where α is the learning rate and η is the momentum factor used to allow the previous weight change to influence the weight change in this time period, t.

(8) Adjust the weights and thresholds in the hidden layer:

$$W_{ji}(t+1) = W_{ji}(t) + \alpha\delta_j h_i + \eta\big(W_{ji}(t) - W_{ji}(t-1)\big) \tag{8}$$

$$\theta_j(t+1) = \theta_j(t) + \alpha\delta_j \tag{9}$$

(9) Repeat steps (2) to (8) on the all pattern pairs until the output layer error is within the specified tolerance for each pattern and for each neuron.

3. Fuzzy logic

System modeling based on conventional mathematical is not well suited for dealing with ill-defined and uncertain systems. By contrast, a fuzzy inference system employing fuzzy *if–then rules* can model the qualitative aspects of human knowledge and reasoning processes without employing precise quantitative analyses. Fuzzy set theory and fuzzy logic were established in 1965 by Zadeh in order to deal with the vagueness and ambiguity associated with human thinking, reasoning, cognition, and perception [17]. After Zadeh's work on fuzzy sets, many theories in fuzzy logic were developed, and *fuzzy modeling or fuzzy identification* has been applied successfully to a number of applications [26–31].

A fuzzy model is one that expresses a complex system in the form of fuzzy implications. In the fuzzy modeling of a process, a fuzzy model is built by using the physical properties of a system, observed data, empirical knowledge, and so on. A typical fuzzy logic system consists of four major components: fuzzification interface, fuzzy rule base, fuzzy inference engine and defuzzification interface. The *fuzzification interface* (*fuzzifier*) converts numerical input data into suitable linguistic terms, which may be viewed as labels of the fuzzy sets. A fuzzy rule represents a fuzzy relation between two fuzzy sets. It takes form such as "If X is A then Y is B". Each fuzzy set is characterized by appropriate membership functions that map each element to a membership value between 0 and 1. A *fuzzy rule base* contains a set of fuzzy rules, where each rule may have multiple inputs and multiple outputs. *Fuzzy inferencing* can be realized by using a series of fuzzy operations. The *defuzzification interface* (*defuzzifier*) combines and converts linguistic conclusions (fuzzy membership functions) into crisp numerical outputs.

Depending on the types of inference operations upon "*if-then rules*", three types of fuzzy inference system have been widely employed in various applications: Mamdani fuzzy models [27], Sugeno fuzzy models [28], and Tsukamoto fuzzy models [29]. The differences between these three fuzzy inference systems lie in the consequents of their fuzzy rules, and thus their aggregation and defuzzification procedures differ accordingly. Strengths, weakness, and other related issues for these systems can be found in Ref. [30].

4. Adaptive neuro-fuzzy inference system (ANFIS)

While fuzzy logic performs an inference mechanism under cognitive uncertainty, computational neural networks offer exciting advantages, such as learning, adaptation, fault-tolerance, parallelism and generalization. To enable a system to deal with cognitive uncertainties in a manner more like humans, neural networks have been engaged with fuzzy logic, creating a new terminology called *neuro-fuzzy* method [30]. Takagi and Hayashi made pioneer augmentation in development of neuro-fuzzy technology in the last decade [31]. Similarly, Jang developed ANFIS (Adaptive Neuro-Fuzzy Inference Systems) in the early 90s [18]. As the name suggests, ANFIS combines the fuzzy qualitative approach with the neural networks adaptive capabilities to achieve a desired performance. ANFIS are fuzzy models put in the framework of adaptive systems to facilitate learning and adaptation. Such system can be trained with no need for the expert knowledge usually required for the design of the standard fuzzy logic.

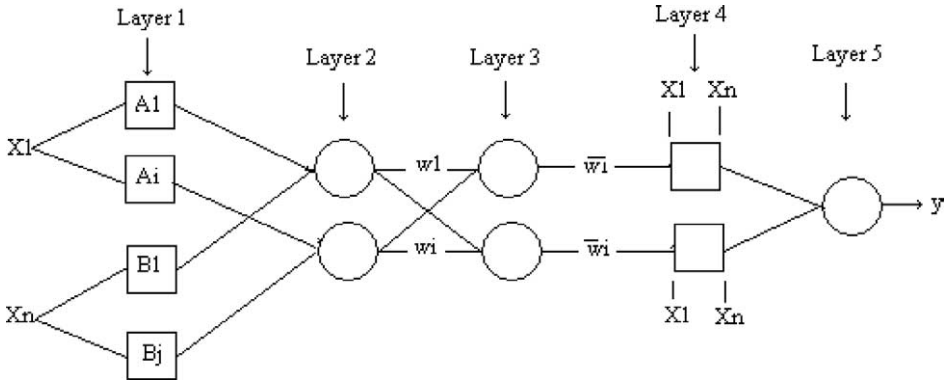

Fig. 3. ANFIS architecture used in this study.

Fig. 3 shows the ANFIS architecture. A first order Sugeno fuzzy model is used as a means of modeling fuzzy rules into desired outputs:

$$\text{if } X1 = A_i \text{ and } Xn = B_j \text{ then } f_i = p_i X1 + q_i Xn + r_i \quad (10)$$

where p_i, q_i and r_i are design parameters to be determined during the training stage. In the presentation, a circle indicates a fixed node whereas a square indicates an adaptive node. An adaptive node means that the parameters are changed during adaptation or training. This architecture is a five-layered feed-forward neural structure, and the functionality of the nodes in these layers is summarized as follows [32,33]:

(1) All the nodes in the first layer are adaptive. Each neuron in this layer corresponds to a linguistic label and the output equals the membership function of this linguistic label:

$$OL1_i = \mu_{Ai}(X1) \quad (11)$$

(2) The nodes in layer 2 are fixed (not adaptive). Each node in this layer estimates the firing strength (w_i) of a rule, which is found from the multiplication of the incoming signal:.

$$OL2_i = w_i = \mu_{Ai}(X1)\mu_{Bj}(Xn) \quad (12)$$

(3) The nodes in layer 3 are also fixed nodes. Each node in this layer estimates the ratio (w_i) of the ith rule's firing strength to sum of the firing strength of all rules, j. They perform a normalization of the firing strength from the previous layer. The output of each node in this layer is given by:

$$OL3_i = \bar{w}_i = \frac{w_i}{\sum_{j=1}^{i} w_i} \quad (13)$$

(4) All the nodes in layer 4 are adaptive nodes. The output of each node in this layer is the product of the previously found relative firing strength of the ith rule (referred to as defuzzifier or consequent parameters) and the rule (a first order polynomial for first order Sugeno model):

$$OL4_i = \bar{w}_i f_i = \bar{w}_i (p_i X1 + q_i Xn + r_i) \quad (14)$$

where p_i, q_i and r_i are design parameters (referred to as consequent parameters since they deal with the then-part of the fuzzy rule).

(5) Layer 5 has only one node, and it performs the function of a simple summer. It computes the overall output as the summation of all incoming signals from layer 4:

$$OL5_i = \sum_{i=1}^{j} \bar{w}_i f_i = \frac{\sum_i w_i f_i}{\sum_i w_i} \quad (15)$$

The results are then defuzzified using a weighted-average procedure.

The ANFIS architecture is not unique. Some layers can be combined and still produce the same output. In this ANFIS architecture, there are two adaptive layers (layers 1 and 4). Layer 1 has modifiable parameters related to the input membership function. The parameters in this layer are called premise parameters. Layer 4 has also three modifiable parameters (p_i, q_i and r_i) pertaining to the first order polynomial. These parameters are called consequent parameters.

The task of the training or learning algorithm for this architecture is to tune all the modifiable parameters to make the ANFIS output match the training data. A training method such as back-propagation or a hybrid learning rule which combines the gradient method and the least squares is employed to find the optimum value for the parameters of the membership functions and a least squares procedure for the linear parameters on the fuzzy rules, in such a way as to minimize the error between the input and the output pairs.

5. Experimental setup and data reduction

The experimental system is designed to study the decay of sinusoidal thermal inlet conditions for transient forced convection in thermally developing and simultaneously developing air flow in a circular duct, and a schematic diagram is given in Fig. 4. The system consists mainly of a suction-type wind tunnel originally designed and built by Brown [6], and experiments were made by Comakli [11] at Miami University, Florida, USA. The main components of the system

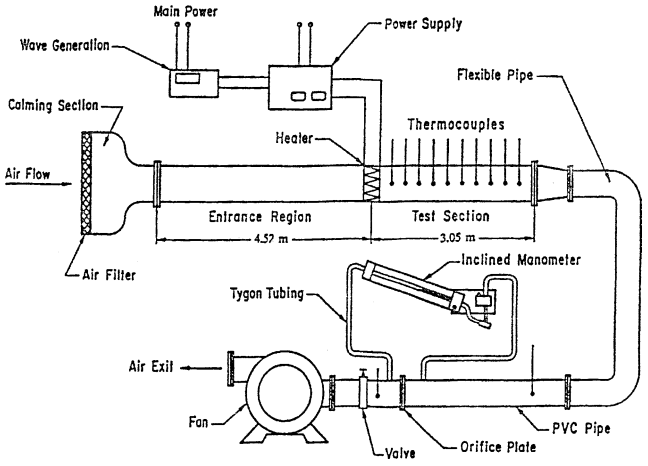

Fig. 4. Experimental system.

are: air filter, calming section, inlet section, electric heater, test section, thermocouples, convergent section, orifice plate, and a fan. Laboratory air is drawn into the apparatus through a filtered bell-mouth inlet geometry. It then passes through a flow development section (4.57 m in length and 7.62 cm in diameter), an electric heater of uniform V-shaped configuration, test section (3.05 m length and 7.62 cm in diameter), flow redevelopment section, orifice plate, main valve and then leaves the flow circuit through the fan, operated in a suction mode. Once the apparatus is properly assembled, the air flow is activated and adjusted for a predetermined flow rate or Reynolds number. This was observed as the pressure drop across the orifice plate. The function generator is switched on, adjusted, and stabilized at a specific periodic frequency of inlet heat input.

Under-steady sustained periodic conditions, the thermal response of the fluid with-time, with respect to the inlet perturbations are obtained from equally spaced beaded-type chromel-constantan thermocouples, installed along the centerline and wall of the test section. To illustrate the dynamic response with-time, a multi-channel strip chart recorder is used in obtaining continuous traces of each thermocouple output as a function of chart speed, pressure drop, probe location and inlet frequency. During this period, the maximum and minimum outputs at individual probes are recorded at each location.

After each experimental run, raw data which consist of millivolt readings from the thermocouples, pressure drop across the orifice plate and test section respectively, in millimeters of liquid column, along with the voltage and current supplied to the heater are recorded. From the measured parameters, mass flow rate ($\dot{m}$), Reynolds numbers (Re_p) and (Re_t), temperature amplitudes with corresponding decay indices and heater power are evaluated.

Under steady-sustained transient conditions, the thermal response of the fluid along the centerline of the circular duct is observed to be periodic oscillations. In this study, amplitudes of the thermal oscillations are defined as one half the difference between maximum and minimum thermocouple outputs, $T_{\max}$ and $T_{\min}$, respectively and expressed as

$$\Delta T = \frac{T_{\max} - T_{\min}}{2} \tag{16}$$

As the inlet temperature varied periodically in time, it was observed that each mode of the thermal oscillation decayed with distance along the duct. Consequently, the absolute value of the exponent in the expression governing temperature amplitude variation with distance, under steady-sustained transient conditions is termed the decay index (α). The decay indices are obtained as slopes of the curves for temperature amplitude versus dimensionless distance, using least squares regression in fitting the experimental results with a 95% confidence limit and the cumulative standard deviation from linearity. In dimensionless form, the amplitude variation along the centerline of the circular duct is defined as

$$\varphi_{\text{amp}} = \frac{\Delta T}{\Delta T_0} = e^{-\alpha(X/D_t)} \tag{17}$$

where X/D_t is the axial dimensionless distance along the duct, ΔT_0 the temperature amplitude measured at the center of the inlet.

In this study, standard beaded-type chromel-constantan thermocouples are used for temperature measurements and a comparison calibration method was adopted. The measurement made with E-type thermocouples usually have a maximum uncertainty of $\pm 0.2\,^{\circ}\text{C}$ within the range of $0\,^{\circ}\text{C}$ to $100\,^{\circ}\text{C}$. The maximum value of the uncertainty associated with the mass flow rate and Reynolds number in turbulent flow was evaluated as $\pm 2.64\%$. The uncertainty associated with decay index (α) was obtained by utilizing least square regression jointly with a 95% confidence interval with the standard deviation from linearly. Based on this method, the maximum uncertainty associated with the computed decay indices is $\pm 5\%$.

The experiments covered Reynolds numbers in the $2528 \leqslant Re \leqslant 4265$ range and inlet heat input in the $0.01 \leqslant \beta \leqslant 0.96$ Hz frequency range. Detailed knowledge on the experimental setup, instrumentation, procedure and measurements can be found in Ref. [11].

6. Results and discussion

6.1. Experimental results

For qualitative analyses of the system's dynamic thermal behavior, the temperature response with-time for predetermined locations along the centerline of the circular duct is presented as a function of inlet frequency and Reynolds number, for thermally developing and simultaneously developing turbulent flows. During the experiments, the temperature at the entrance was specified as a sinusoidal oscillation with a specified frequency. The thermal response with time, and amplitude variation of the centerline thermal oscillations

Table 1
Experimental temperature amplitude for circular duct in the hydrodynamically developed and thermally developing flow

X/D_t	ΔT [°C]					
	$Re = 3068$ $\beta = 0.03$ Hz	$Re = 3069$ $\beta = 0.06$ Hz	$Re = 3068$ $\beta = 0.12$ Hz	$Re = 3068$ $\beta = 0.24$ Hz	$Re = 3069$ $\beta = 0.48$ Hz	$Re = 3061$ $\beta = 0.96$ Hz
1	5.508079	4.3425	2.358107	0.634339	0.226191	0.131823
3	5.421759	4.27692	2.307767	0.632339	0.215811	0.126163
6	5.292279	4.17855	2.232257	0.629339	0.200241	0.117673
9	5.162799	4.08018	2.156747	0.626339	0.184671	0.109183
12	5.033319	3.98181	2.081237	0.623339	0.169101	0.100693
15	4.903839	3.88344	2.005727	0.620339	0.153531	0.092203
18	4.774359	3.78507	1.930217	0.617339	0.137961	0.083713
21	4.644879	3.6867	1.854707	0.614339	0.122391	0.075223
24	4.515399	3.58833	1.779197	0.611339	0.106821	0.066733
27	4.385919	3.48996	1.703687	0.608339	0.091251	0.058243
30	4.256439	3.39159	1.628177	0.605339	0.075681	0.049753
33	4.126959	3.29322	1.552667	0.602339	0.060111	0.041263
36	3.997479	3.19485	1.477157	0.599339	0.044541	0.032773
39	3.867999	3.09648	1.401647	0.596339	0.028971	0.024283

Table 2
Experimental temperature amplitude for circular duct in the hydrodynamically and thermally developing (simultaneously developing) flow

X/D_t	ΔT [°C]					
	$Re = 3046$ $\beta = 0.03$ Hz	$Re = 3045$ $\beta = 0.06$ Hz	$Re = 3048$ $\beta = 0.12$ Hz	$Re = 3049$ $\beta = 0.24$ Hz	$Re = 3049$ $\beta = 0.48$ Hz	$Re = 3050$ $\beta = 0.96$ Hz
1	5.541988	4.350546	2.364915	0.636127	0.252928	0.138746
3	5.499351	3.798271	2.234005	0.628585	0.212195	0.130597
6	5.450015	3.764223	1.992028	0.612258	0.204115	0.122416
9	5.132332	3.513217	1.720977	0.587339	0.195835	0.114213
12	5.017992	3.438298	1.688491	0.571166	0.187709	0.114244
15	4.986904	3.310014	1.65609	0.489638	0.15506	0.114188
18	3.665484	3.009877	1.534709	0.473343	0.130586	0.106097
21	3.502781	2.51461	1.315222	0.408358	0.12245	0.097994
24	3.267833	2.393165	1.274288	0.38383	0.12251	0.089866
27	3.072348	2.034618	0.997136	0.34321	0.114345	0.065333
30	2.755378	1.887952	0.923974	0.326894	0.10629	0.065386
33	2.731644	1.757864	0.916063	0.310739	0.098126	0.057223
36	2.633205	1.782418	0.89963	0.261711	0.073623	0.057223
39	2.520044	1.668782	0.818277	0.240939	0.063627	0.040916

are expressed as function of the dimensionless distance at various values of Reynolds number and inlet frequency. Amplitudes of the thermal oscillations are defined as one half the difference between maximum and minimum thermocouple outputs (Eq. (16)).

Tables 1 and 2 show the experimental temperature amplitudes for the thermally developing and simultaneously developing flows for the range of inlet frequencies considered, respectively. The experimental results can be summarized as follows [11]:

(1) The centerline temperature amplitudes at the upstream end were much greater than those at the downstream end.
(2) The amplitude of the oscillations is observed to decay with small, but increasing phase lag with increasing distance from the inlet.
(3) For high inlet frequencies, the amplitude of the thermal oscillation along the centerline is observed to be negligible in both thermally and simultaneously developing flows.
(4) The thermal response along the centerline changed periodically with approximately the same frequency as that imposed at the inlet.
(5) For given Reynolds number, the temperature amplitude is observed to decrease by 82 and 88% for fully developed and simultaneously developing flows, respectively over an inlet frequency range of 0.03–0.96 Hz.
(6) At a given value of the inlet frequency, the dimensionless temperature amplitude at a point downstream depends on the Reynolds number and the dominant mode of heat transfer.
(7) The effects of inlet frequency on the thermal response of the fluid within the temperature field are observed to be more dominant in simultaneously developing flows when compared to fully developed flows.

The results of the experimental investigation can be found in detail in Ref. [11].

6.2. ANFIS results

To approach adopted in this investigation was to model the temperature amplitude, ΔT, as a function of three variables namely,

(i) X/D_t, the dimensionless distance,
(ii) Re, Reynolds number, and
(iii) β, the heating frequency.

ANFIS was used to train and validate the neural network and to generate the fuzzy rules. Fig. 5 shows a typical three-input network used in this application. Based on the experimental data [11], the dimensionless distance, Reynolds number and the heating frequency were chosen as the input, and the temperature amplitude was used as the output.

The training and test performances of the ANFIS are presented in Table 3. A three-input, first order, Sugeno fuzzy inference system with 16 rules was used. The number of rules was selected as 16 after trying various numbers of rules, i.e., 4, 6, 9, 16 and 20. Sixteen membership functions were chosen for each input, and the membership function parameters were tuned using a hybrid algorithm (mixed least squares and back-propagation). All of the membership functions of the input variables were of the Gaussian type, and the premise parameter sub-spaces were determined by using k-means clustering of the training data set. The aim of the training data set is to construct a network for achieving a desired mapping that is regulated by the data set consisting of desired input–output pairs of a target system. With a better set of training patterns it is possible to predict the output with high accuracy. In order to verify the generation of the model, all of the data were divided into two categories: half of them for the training set, the other half for the test set. The ANFIS was set for training, and the tuning algorithm modified the ANFIS parameters to match the training data. After having been verified by the test data set, the temperature amplitudes were estimated using the above neuro-fuzzy algorithm procedure.

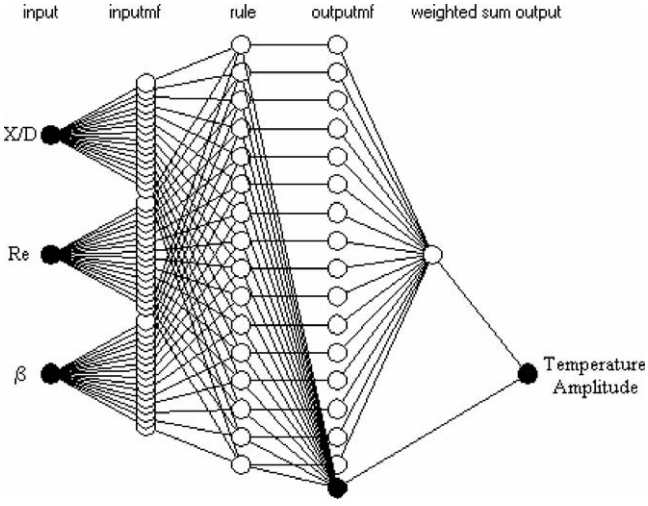

Fig. 5. A three-input, first order, Sugeno fuzzy inference system with 16 rules used in this study.

The speed of learning is governed by the learning rate. Learning rate affects the convergence speed and stability of the weights during learning. If the learning rate is increased too much, learning becomes unstable; the net oscillates back and forth across the error minimum. Learning rate was selected as 0.01 for thermally and simultaneously developing flow. The training error is the difference between the training data output value and the output of the fuzzy inference system corresponding to the same training data input value. The training error was found to be equal to 0.0035 and 0.0088 for thermally and simultaneously developing flow, respectively. Test errors, which assess the variance between measured and predicted values were of the same order in magnitude for thermally and simultaneously developing flow, as seen in Table 3. Epochs were setted as 50 and 60 for thermally and simultaneously developing flow, respectively.

The predicted temperature amplitudes obtained with the ANFIS in addition to the experimental temperature amplitudes for different heating frequencies in the hydrodynamically developed and thermally developing flow are shown in Table 4. This table includes also the error difference (Δ) and error deviation ($\Delta\%$). In the present work, the Δ and $\Delta\%$ are evaluated as

$$(\Delta T)_i = T_i^{\text{exp}} - T_i^{\text{pred}} \tag{18}$$

$$(\Delta T\%)_i = \frac{T_i^{\text{exp}} - T_i^{\text{pred}}}{T_i^{\text{exp}}} \times 100 \tag{19}$$

where ‘exp’ and ‘pred’ stand for experimental and calculated values, respectively. A plot of the experimental temperature amplitude against dimensionless distance is given in Fig. 6, which includes also the predicted values obtained with the ANFIS. A maximum error deviation confined to less than

Table 3
Training and test performances of ANFIS

Flow type	Train algorithm	Learning rate	Training error	Test error	Epochs	Rules for each input
Thermally developing	Hybrid	0.01	0.0035014	0.03290	50	16
Simultaneously developing	Hybrid	0.01	0.00875	0.02680	60	16

Table 4
Experimental and predicted temperature amplitudes obtained with the ANFIS, error differences, error deviations for circular duct in the hydrodynamically developed and thermally developing flow

X/D_t	$Re = 3068$, $\beta = 0.03$				$Re = 3069$, $\beta = 0.06$				$Re = 3068$, $\beta = 0.12$			
	Exp. T_{amp} [°C]	Pre. T_{amp} [°C]	ΔT	ΔT%	Exp. T_{amp} [°C]	Pre. T_{amp} [°C]	ΔT	ΔT%	Exp. T_{amp} [°C]	Pre. T_{amp} [°C]	ΔT	ΔT%
1	5.508079	5.92	0.411921	7.478487509	4.3425	4.59	0.2475	5.699481865	2.358107	2.4	0.041893	1.776552124
3	5.421759	5.83	0.408241	7.529678099	4.27692	4.5	0.22308	5.215903033	2.307767	2.34	0.032233	1.396718126
6	5.292279	5.65	0.357721	6.759299727	4.17855	4.35	0.17145	4.103097965	2.232257	2.26	0.027743	1.242822847
9	5.162799	5.42	0.257201	4.98181316	4.08018	4.2	0.11982	2.936635148	2.156747	2.19	0.033253	1.541812739
12	5.033319	5.17	0.136681	2.715524289	3.98181	4.05	0.06819	1.712537765	2.081237	2.1	0.018763	0.901531157
15	4.903839	4.95	0.046161	0.941323726	3.88344	3.91	0.02656	0.683929712	2.005727	2.01	0.004273	0.21303996
18	4.774359	4.79	0.015641	0.327604187	3.78507	3.79	0.00493	0.130248582	1.930217	1.94	0.009783	0.506834206
21	4.644879	4.65	0.005121	0.11025045	3.6867	3.69	0.0033	0.089510945	1.854707	1.86	0.005293	0.285382004
24	4.515399	4.51	0.005399	0.119568614	3.58833	3.59	0.00167	0.046539755	1.779197	1.78	0.000803	0.04513272
27	4.385919	4.38	0.005919	0.134954613	3.48996	3.49	4E–05	0.001146145	1.703687	1.7	0.003687	0.216412991
30	4.256439	4.26	0.003561	0.083661483	3.39159	3.39	0.00159	0.046880667	1.628177	1.63	0.001823	0.111965714
33	4.126959	4.13	0.003041	0.073686218	3.29322	3.29	0.00322	0.097776644	1.552667	1.55	0.002667	0.171768963
36	3.997479	3.99	0.007479	0.187092915	3.19485	3.19	0.00485	0.151806814	1.477157	1.48	0.002843	0.192464308
39	3.867999	3.87	0.002001	0.051732175	3.09648	3.1	0.00352	0.113677466	1.401647	1.4	0.001647	0.117504621
X/D_t	$Re = 3068$, $\beta = 0.24$				$Re = 3069$, $\beta = 0.48$				$Re = 3061$, $\beta = 0.96$			
	Exp. T_{amp} [°C]	Pre. T_{amp} [°C]	ΔT	ΔT%	Exp. T_{amp} [°C]	Pre. T_{amp} [°C]	ΔT	ΔT%	Exp. T_{amp} [°C]	Pre. T_{amp} [°C]	ΔT	ΔT%
1	0.634339	0.649	0.014661	2.311224755	0.226191	0.233	0.006809	3.010287766	0.131823	0.132	0.000177	0.134270954
3	0.632339	0.635	0.002661	0.42081858	0.215811	0.221	0.005189	2.404418681	0.126163	0.126	0.000163	0.129197942
6	0.629339	0.637	0.007661	1.217308954	0.200241	0.203	0.002759	1.377839703	0.117673	0.118	0.000327	0.277888726
9	0.626339	0.635	0.008661	1.382797495	0.184671	0.186	0.001329	0.719658203	0.109183	0.109	0.000183	0.16760851
12	0.623339	0.623	0.000339	0.054384532	0.169101	0.17	0.000899	0.53163494	0.100693	0.101	0.000307	0.304887132
15	0.620339	0.619	0.001339	0.215849721	0.153531	0.154	0.000469	0.305475767	0.092203	0.0924	0.000197	0.213658992
18	0.617339	0.622	0.004661	0.755014668	0.137961	0.138	3.9E–05	0.028268859	0.083713	0.0838	8.7E–05	0.103926511
21	0.614339	0.612	0.002339	0.380734415	0.122391	0.121	0.001391	1.136521476	0.075223	0.0753	7.7E–05	0.102362309
24	0.611339	0.607	0.004339	0.709753508	0.106821	0.106	0.000821	0.768575467	0.066733	0.0666	0.000133	0.199301695
27	0.608339	0.61	0.001661	0.273038553	0.091251	0.092	0.000749	0.820812923	0.058243	0.0583	5.7E–05	0.097865838
30	0.605339	0.605	0.000339	0.056001678	0.075681	0.0761	0.000419	0.553639619	0.049753	0.0497	5.3E–05	0.10652624
33	0.602339	0.598	0.004339	0.720358469	0.060111	0.0591	0.001011	1.681888506	0.041263	0.0413	3.7E–05	0.08966871
36	0.599339	0.595	0.004339	0.723964234	0.044541	0.0436	0.000941	2.112660246	0.032773	0.0328	2.7E–05	0.08238489
39	0.596339	0.593	0.003339	0.559916423	0.028971	0.0295	0.000529	1.825963895	0.024283	0.0243	1.7E–05	0.070007824

Table 5
Predicted temperature amplitudes obtained with the ANFIS for different heating frequencies for circular duct in the hydrodynamically developed and thermally developing flow

X/D_t	$Re = 3068$ $\beta = 0.045$ Hz	$Re = 3069$ $\beta = 0.090$ Hz	$Re = 3068$ $\beta = 0.18$ Hz	$Re = 3068$ $\beta = 0.36$ Hz	$Re = 3069$ $\beta = 0.72$ Hz
1	4.71	3.21	0.925	0.99	1.04
3	4.63	3.14	0.91	0.987	1.09
6	4.51	3.04	0.891	0.978	1.16
9	4.4	2.95	0.892	0.973	1.21
12	4.29	2.87	0.871	0.968	1.23
15	4.21	2.8	0.86	0.966	1.17
18	4.14	2.75	0.852	0.963	1.01
21	4.06	2.68	0.842	0.851	0.761
24	3.95	2.6	0.856	0.713	0.557
27	3.83	2.54	0.862	0.634	0.492
30	3.71	2.49	0.817	0.644	0.532
33	3.58	2.43	0.766	0.723	0.612
36	3.45	2.34	0.705	0.825	0.689
39	3.34	2.27	0.666	0.913	0.746

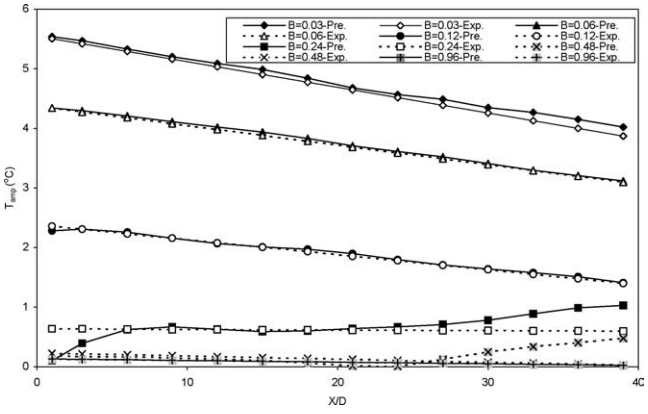

Fig. 6. Experimental and predicted temperature amplitudes obtained with the ANFIS in the hydrodynamically developed and thermally developing flow.

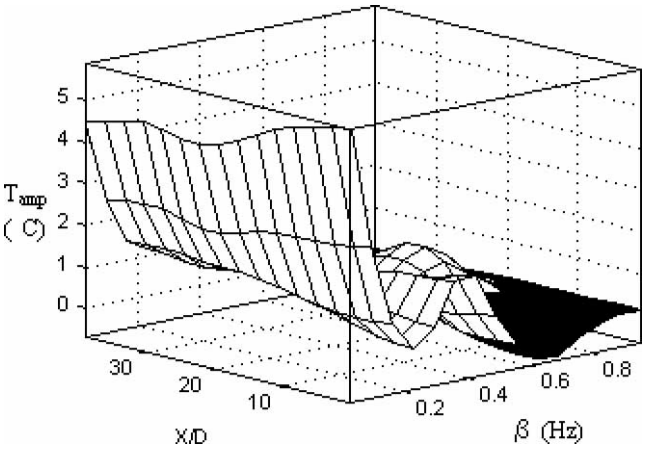

Fig. 7. Overall input–output surface for hydrodynamically developed and thermally developing flow.

7.52% was obtained, while the average absolute deviation (AAD%) was 1.076. AAD% are evaluated as

$$\mathrm{AAD\%} = \frac{1}{\mathrm{NPT}} \sum_{i=1}^{\mathrm{NPT}} |\Delta T\%|_i \tag{20}$$

where NPT is the number of points. In general, the matching of the experimental and predicted values in each case was acceptable. Therefore the neuro-fuzzy could be used to predict the temperature amplitude distribution with an acceptable level of accuracy.

Using the same neuro-fuzzy algorithm procedure, temperature amplitude for some different heating frequencies are predicted and presented in Table 5. Overall input–output surface for the hydrodynamically developed and thermally developing flow obtained with the ANFIS is given in Fig. 7. In addition to providing to predict the experimental temperature amplitudes, the overall input–output surface proves also that

(i) the centerline temperature amplitudes at the upstream end are much greater than those at the downstream end,
(ii) the amplitude of the oscillations decays with small, but increasing phase lag with increasing distance from the inlet, and
(iii) for high inlet frequencies, the amplitude of the thermal oscillation along the centerline is negligible in both thermally and simultaneously developing flows.

The ANFIS was also employed to predict temperature amplitudes for simultaneously developing flows for different inlet frequencies. Table 6 and Fig. 8 show the comparison between the ANFIS prediction and the experimental measurements. An examination of Table 6 shows that the maximum error deviation (Δ) and average absolute deviation ($\Delta\%$) are confined to less than 14.37 and 3.7%, respectively. These results show that good predictions are achieved for the temperature amplitudes of the simultaneously developing flows. Using the same neuro-fuzzy algorithm procedure, temperature amplitudes for some different heating frequencies are predicted and presented in Table 7. Fig. 9 presents

Table 6
Experimental and predicted temperature amplitudes obtained with the ANFIS, error differences, error deviations for circular duct in the hydrodynamically and thermally developing (simultaneously developing) flow

X/D_t	$Re = 3046$, $\beta = 0.03$				$Re = 3045$, $\beta = 0.06$				$Re = 3048$, $\beta = 0.12$			
	Exp. T_{amp} [°C]	Pre. T_{amp} [(°C]	ΔT	$\Delta T\%$	Exp. T_{amp} [°C]	Pre. T_{amp} [°C]	ΔT	$\Delta T\%$	Exp. T_{amp} [°C]	Pre. T_{amp} [°C]	ΔT	$\Delta T\%$
1	5.541988	5.57	0.028012	0.505450391	4.350546	4.74	0.389454	8.951841907	2.364915	2.41	0.045085	1.906411013
3	5.499351	5.5	0.000649	0.011801393	3.798271	3.65	0.148271	3.903644579	2.234005	2.26	0.025995	1.163605274
6	5.450015	5.39	0.060015	1.10118963	3.764223	3.5	0.264223	7.019323775	1.992028	2.05	0.057972	2.910200057
9	5.132332	5.27	0.137668	2.682367392	3.513217	3.35	0.163217	4.645798993	1.720977	1.87	0.149023	8.659209275
12	5.017992	5.09	0.072008	1.434996309	3.438298	3.16	0.278298	8.094062818	1.688491	1.72	0.031509	1.866104113
15	4.986904	4.72	0.266904	5.352098216	3.310014	3.77	0.459986	13.89679923	1.65609	1.61	0.04609	2.783061307
18	3.665484	4.01	0.344516	9.398922489	3.009877	3.04	0.030123	1.000805016	1.534709	1.5	0.034709	2.261601385
21	3.502781	3.39	0.112781	3.21975596	2.51461	2.43	0.08461	3.36473648	1.315222	1.38	0.064778	4.925252163
24	3.267833	3.14	0.127833	3.911858409	2.393165	2.16	0.233165	9.742955459	1.274288	1.19	0.084288	6.614517283
27	3.072348	3.03	0.042348	1.378359483	2.034618	2.02	0.014618	0.718464105	0.997136	1.03	0.032864	3.295839284
30	2.755378	2.9	0.144622	5.248717236	1.887952	1.89	0.002048	0.108477334	0.923974	0.93	0.006026	0.652182854
33	2.731644	2.76	0.028356	1.038056204	1.757864	1.78	0.022136	1.259255551	0.916063	0.88	0.036063	3.936737975
36	2.633205	2.61	0.023205	0.881245478	1.782418	1.71	0.072418	4.062907803	0.89963	0.86	0.03963	4.405144337
39	2.520044	2.49	0.030044	1.192201406	1.668782	1.71	0.041218	2.469945146	0.818277	0.84	0.021723	2.6547245
X/D_t	$Re = 3049$, $\beta = 0.24$				$Re = 3049$, $\beta = 0.48$				$Re = 3050$, $\beta = 0.96$			
	Exp. T_{amp} [°C]	Pre. T_{amp} [°C]	ΔT	$\Delta T\%$	Exp. T_{amp} [°C]	Pre. T_{amp} [°C]	ΔT	$\Delta T\%$	Exp. T_{amp} [°C]	Pre. T_{amp} [°C]	ΔT	$\Delta T\%$
1	0.636127	0.64	0.003873	0.608840687	0.252928	0.226	0.026928	10.6465081	0.138746	0.141	0.002254	1.624551338
3	0.628585	0.632	0.003415	0.543283725	0.212195	0.213	0.000805	0.379368034	0.130597	0.13	0.000597	0.457131481
6	0.612258	0.618	0.005742	0.93783993	0.204115	0.195	0.009115	4.465619871	0.122416	0.119	0.003416	2.790484904
9	0.587339	0.597	0.009661	1.644876298	0.195835	0.181	0.014835	7.575254679	0.114213	0.115	0.000787	0.689063417
12	0.571166	0.56	0.011166	1.954948299	0.187709	0.172	0.015709	8.368804905	0.114244	0.116	0.001756	1.537061027
15	0.489638	0.508	0.018362	3.750117434	0.15506	0.155	6E-05	0.038694699	0.114188	0.115	0.000812	0.711107997
18	0.473343	0.457	0.016343	3.452675966	0.130586	0.13	0.000586	0.44874642	0.106097	0.107	0.000903	0.851107948
21	0.408358	0.415	0.006642	1.62651399	0.12245	0.118	0.00445	3.634136382	0.097994	0.095	0.002994	3.055289099
24	0.38383	0.381	0.00283	0.737305578	0.12251	0.116	0.00651	5.31385193	0.089866	0.084	0.005866	6.527496495
27	0.34321	0.349	0.00579	1.687013782	0.114345	0.113	0.001345	1.176264813	0.065333	0.074	0.008667	13.26588401
30	0.326894	0.318	0.008894	2.720759635	0.10629	0.106	0.00029	0.272838461	0.065386	0.064	0.001386	2.119719818
33	0.310739	0.288	0.022739	7.317716798	0.098126	0.093	0.005126	5.223895807	0.057223	0.056	0.001223	2.137252503
36	0.261711	0.261	0.000711	0.271673716	0.073623	0.076	0.002377	3.228610624	0.057223	0.049	0.008223	14.37009594
39	0.240939	0.236	0.004939	2.049896447	0.063627	0.055	0.008627	13.55870935	0.040916	0.046	0.005084	12.42545703

Table 7
Predicted temperature amplitudes obtained with the ANFIS for different heating frequencies for circular duct in the hydrodynamically and thermally developing flow

X/D_t	$Re = 3046$ $\beta = 0.045$ Hz	$Re = 3045$ $\beta = 0.090$ Hz	$Re = 3048$ $\beta = 0.18$ Hz	$Re = 3049$ $\beta = 0.36$ Hz	$Re = 3049$ $\beta = 0.72$ Hz
1	5.23	2.35	1.53	1.35	0.465
3	5.15	2.02	1.46	1.33	0.437
6	5.04	1.54	1.36	1.29	0.393
9	4.91	1.19	1.27	1.25	0.342
12	4.73	1.15	1.19	1.22	0.268
15	4.35	1.64	1.14	1.22	0.124
18	3.6	1.45	1.14	1.24	0.182
21	2.95	1.38	1.24	1.24	0.545
24	2.7	1.58	1.47	1.18	0.627
27	2.59	1.23	1.8	1.03	0.562
30	2.48	1.02	2.11	0.812	0.514
33	2.35	0.891	2.34	0.595	0.502
36	2.22	0.829	2.48	0.433	0.51
39	2.11	0.833	2.57	0.332	0.531

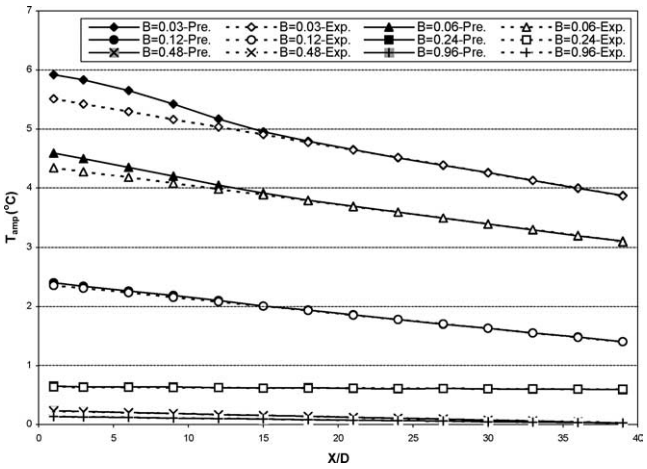

Fig. 8. Experimental and predicted temperature amplitudes obtained with the ANFIS in the hydrodynamically and thermally developing flow

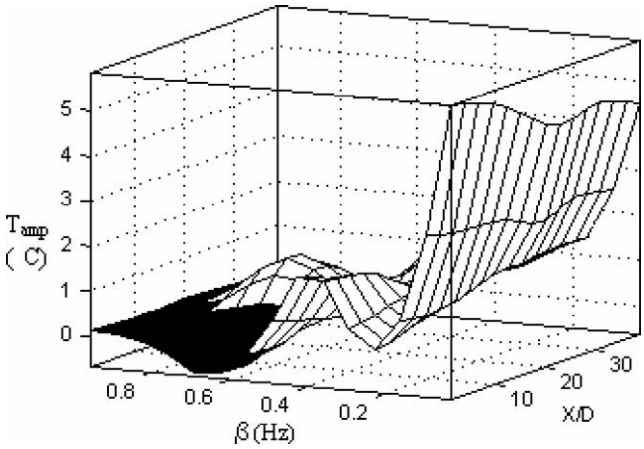

Fig. 9. Overall input–output surface for hydrodynamically and thermally developing flow.

overall input–output surface for simultaneously developing flow.

6.3. Comparison of the ANFIS results with other techniques

In order to check whether the predictions of transient heat transfer can be done with traditional non-AI techniques or pure neural network without using hybrid neuro-fuzzy approach, a multiple linear regression analysis and a neural network analysis were used. Presenting these alternative approaches and comparing the results could shed more light on the difficulty of the problem and the power of non-traditional methods in solving it.

It is well known that the performance of an artificial intelligence technique depends on various parameters such as the speed of learning, the speed of convergence, the complexity of tuning/learning algorithm, the accuracy, the configuration of networks etc. For instance, the speed of learning can be improved by using appropriate number of hidden nodes, the global learning coefficient, and the momentum factor. In the present work, the comparison of the three approaches was made on the basis of the accuracy, the complexity of tuning/learning algorithm, standard deviation, train and test performance.

Multiple linear regression analysis is usually used to summarize data as well as study relations between variables [34]. Stepwise regression is basically a combination of backward and forward procedures and is probably the most commonly used method [35,36]. In this method, the first variable is selected in the same manner as in the forward selection. If the variables fail to meet the entry requirements, the procedure terminates with no independent variables entering into the equation. If it passes the criterion, the second variable based on the highest partial correlation is selected. If it passes the entry criterion, it also enters the equation. After the first variable is entered, stepwise selection differs from forward selection: the first variable is examined to see whether it should be removed according to the removal criterion as in backward elimination. In the next step, variables not in the equation are examined for removal. Variables are removed

Table 8
Comparison of the predicted temperatures obtained with the ANFIS, neural network and multiregression methods for circular duct in the hydrodynamically developed and thermally developing flow

X/D_t	$Re = 3068$, $\beta = 0.03$ Hz				$Re = 3069$, $\beta = 0.06$ Hz				$Re = 3068$, $\beta = 0.12$ Hz			
	Exp. T_{amp} [°C]	Pred. T_{amp} [°C]			Exp. T_{amp} [°C]	Pred. T_{amp} [°C]			Exp. T_{amp} [°C]	Pred. T_{amp} [°C]		
		ANFIS	Neural network	Multi regression		ANFIS	Neural network	Multi regression		ANFIS	Neural network	Multi regression
1	5.508079	5.92	5.455768	4.41074	4.3425	4.59	4.379260	3.68648	2.358107	2.4	2.385521	3.71396
3	5.421759	5.83	5.373071	4.37074	4.27692	4.5	4.311129	3.64648	2.307767	2.34	2.346013	2.78492
6	5.292279	5.65	5.248456	4.31074	4.17855	4.35	4.208591	3.58648	2.232257	2.26	2.285878	4.37074
9	5.162799	5.42	5.123118	4.25074	4.08018	4.2	4.105595	0.33484	2.156747	2.19	2.224623	3.67396
12	5.033319	5.17	4.996999	4.19074	3.98181	4.05	4.002076	3.46648	2.081237	2.1	2.162156	2.74492
15	4.903839	4.95	4.870031	4.13074	3.88344	3.91	3.897956	0.21484	2.005727	2.01	2.098374	4.31074
18	4.774359	4.79	4.742133	4.07074	3.78507	3.79	3.793146	3.40648	1.930217	1.94	2.033165	3.61396
21	4.644879	4.65	4.613208	4.01074	3.6867	3.69	3.687545	0.15484	1.854707	1.86	1.966405	2.68492
24	4.515399	4.51	4.483149	3.95074	3.58833	3.59	3.581038	3.34648	1.779197	1.78	1.897960	4.25074
27	4.385919	4.38	4.351835	3.89074	3.48996	3.49	3.473500	0.09484	1.703687	1.7	1.827684	3.55396
30	4.256439	4.26	4.219131	3.83074	3.39159	3.39	3.364794	3.28648	1.628177	1.63	1.755422	2.62492
33	4.126959	4.13	4.084892	3.77074	3.29322	3.29	3.254769	0.03484	1.552667	1.55	1.681008	4.19074
36	3.997479	3.99	3.948961	3.71074	3.19485	3.19	3.143265	3.22648	1.477157	1.48	1.604266	3.49396
39	3.867999	3.87	3.811172	3.65074	3.09648	3.1	3.030111	−0.02516	1.401647	1.4	1.525011	2.56492
X/D_t	$Re = 3068$, $\beta = 0.24$ Hz				$Re = 3069$, $\beta = 0.48$ Hz				$Re = 3061$, $\beta = 0.96$ Hz			
	Exp. T_{amp} [°C]	Pred. T_{amp} [°C]			Exp. T_{amp} [°C]	Pred. T_{amp} [°C]			Exp. T_{amp} [°C]	Pred. T_{amp} [°C]		
		ANFIS	Neural network	Multi regression		ANFIS	Neural network	Multi regression		ANFIS	Neural network	Multi regression
1	0.634339	0.649	0.623374	2.78492	0.226191	0.233	0.177264	0.43484	0.131823	0.132	0.102602	0.65468
3	0.632339	0.635	0.617108	4.37074	0.215811	0.221	0.185369	3.64648	0.126163	0.126	0.108588	0.61468
6	0.629339	0.637	0.606065	3.67396	0.200241	0.203	0.195772	0.39484	0.117673	0.118	0.114746	0.55468
9	0.626339	0.635	0.592986	2.74492	0.184671	0.186	0.204039	3.58648	0.109183	0.109	0.117429	0.49468
12	0.623339	0.623	0.577797	4.31074	0.169101	0.17	0.210125	0.33484	0.100693	0.101	0.116531	0.55468
15	0.620339	0.619	0.560411	3.61396	0.153531	0.154	0.213979	3.52648	0.092203	0.0924	0.111932	0.49468
18	0.617339	0.622	0.540732	2.68492	0.137961	0.138	0.215538	0.27484	0.083713	0.0838	0.103504	0.43468
21	0.614339	0.612	0.518654	4.25074	0.122391	0.121	0.214731	3.46648	0.075223	0.0753	0.091107	0.37468
24	0.611339	0.607	0.494062	3.55396	0.106821	0.106	0.211475	0.21484	0.066733	0.0666	0.074595	0.31468
27	0.608339	0.61	0.466827	2.62492	0.091251	0.092	0.205680	3.40648	0.058243	0.0583	0.053809	0.25468
30	0.605339	0.605	0.436813	4.19074	0.075681	0.0761	0.197243	0.15484	0.049753	0.0497	0.028588	0.19468
33	0.602339	0.598	0.403873	3.49396	0.060111	0.0591	0.186051	3.34648	0.041263	0.0413	−0.001238	0.13468
36	0.599339	0.595	0.367851	2.56492	0.044541	0.0436	0.171982	0.09484	0.032773	0.0328	−0.035841	0.07468
39	0.596339	0.593	0.328581	4.13074	0.028971	0.0295	0.154903	3.28648	0.024283	0.0243	−0.075395	0.01468

Table 9
Comparison of the predicted temperatures obtained with the ANFIS, neural network and multiregression methods for circular duct in the hydrodynamically and thermally developing (simultaneously developing) flow

X/D_t	$Re = 3046$, $\beta = 0.03$ Hz				$Re = 3045$, $\beta = 0.06$ Hz				$Re = 3048$, $\beta = 0.12$ Hz			
	Exp. T_{amp} [°C]	Pred. T_{amp} [°C]			Exp. T_{amp} [°C]	Pred. T_{amp} [°C]			Exp. T_{amp} [°C]	Pred. T_{amp} [°C]		
		ANFIS	Neural network	Multi regression		ANFIS	Neural network	Multi regression		ANFIS	Neural network	Multi regression
1	5.541988	5.57	5.568909	3.36188	4.350546	4.74	4.455783	2.64794	2.364915	2.41	2.199947	1.18976
3	5.499351	5.5	5.354130	3.28188	3.798271	3.65	4.257783	2.56794	2.234005	2.26	2.099898	1.10976
6	5.450015	5.39	5.040906	3.16188	3.764223	3.5	3.970104	2.44794	1.992028	2.05	1.956977	0.98976
9	5.132332	5.27	4.738645	3.04188	3.513217	3.35	3.693707	2.32794	1.720977	1.87	1.822325	0.86976
12	5.017992	5.09	4.447542	2.92188	3.438298	3.16	3.428646	2.20794	1.688491	1.72	1.695589	0.74976
15	4.986904	4.72	4.167722	2.80188	3.310014	3.77	3.174912	2.08794	1.65609	1.61	1.576417	0.62976
18	3.665484	4.01	3.899244	2.68188	3.009877	3.04	2.932443	1.96794	1.534709	1.5	1.464457	0.50976
21	3.502781	3.39	3.642108	2.56188	2.51461	2.43	2.701125	1.84794	1.315222	1.38	1.359365	0.38976
24	3.267833	3.14	3.396258	2.44188	2.393165	2.16	2.480800	1.72794	1.274288	1.19	1.260801	0.26976
27	3.072348	3.03	3.161586	2.32188	2.034618	2.02	2.271270	1.60794	0.997136	1.03	1.168435	0.14976
30	2.755378	2.9	2.937939	2.20188	1.887952	1.89	2.072303	1.48794	0.923974	0.93	1.081942	0.02976
33	2.731644	2.76	2.725126	2.08188	1.757864	1.78	1.883635	1.36794	0.916063	0.88	1.001010	−0.09024
36	2.633205	2.61	2.522917	1.96188	1.782418	1.71	1.704980	1.24794	0.89963	0.86	0.925336	−0.21024
39	2.520044	2.49	2.331053	1.84188	1.668782	1.71	1.536030	1.12794	0.818277	0.84	0.854627	−0.33024
X/D_t	$Re = 3049$, $\beta = 0.24$ Hz				$Re = 3049$, $\beta = 0.48$ Hz				$Re = 3050$, $\beta = 0.96$ Hz			
	Exp. T_{amp} [°C]	Pred. T_{amp} [°C]			Exp. T_{amp} [°C]	Pred. T_{amp} [°C]			Exp. T_{amp} [°C]	Pred. T_{amp} [°C]		
		ANFIS	Neural network	Multi regression		ANFIS	Neural network	Multi regression		ANFIS	Neural network	Multi regression
1	0.636127	0.64	0.652114	0.44552	0.252928	0.226	0.096890	0.39704	0.138746	0.141	0.215105	−0.41992
3	0.628585	0.632	0.622639	0.36552	0.212195	0.213	0.095828	0.31704	0.130597	0.13	0.215757	−0.49992
6	0.612258	0.618	0.581013	0.24552	0.204115	0.195	0.094456	0.19704	0.122416	0.119	0.216716	−0.61992
9	0.587339	0.597	0.542320	0.12552	0.195835	0.181	0.093328	0.07704	0.114213	0.115	0.217654	−0.73992
12	0.571166	0.56	0.506374	0.00552	0.187709	0.172	0.092424	−0.04296	0.114244	0.116	0.218571	−0.85992
15	0.489638	0.508	0.472999	−0.11448	0.15506	0.155	0.091726	−0.16296	0.114188	0.115	0.219469	−0.97992
18	0.473343	0.457	0.442030	−0.23448	0.130586	0.13	0.091215	−0.28296	0.106097	0.107	0.220346	−1.09992
21	0.408358	0.415	0.413313	−0.35448	0.12245	0.118	0.090877	−0.40296	0.097994	0.095	0.221204	−1.21992
24	0.38383	0.381	0.386698	−0.47448	0.12251	0.116	0.090697	−0.52296	0.089866	0.084	0.222043	−1.33992
27	0.34321	0.349	0.362049	−0.59448	0.114345	0.113	0.090659	−0.64296	0.065333	0.074	0.222864	−1.45992
30	0.326894	0.318	0.339234	−0.71448	0.10629	0.106	0.090752	−0.76296	0.065386	0.064	0.223666	−1.57992
33	0.310739	0.288	0.318133	−0.83448	0.098126	0.093	0.090963	−0.88296	0.057223	0.056	0.224450	−1.69992
36	0.261711	0.261	0.298628	−0.95448	0.073623	0.076	0.091282	−1.00296	0.057223	0.049	0.225217	−1.81992
39	0.240939	0.236	0.280614	−1.07448	0.063627	0.055	0.091698	−1.12296	0.040916	0.046	0.225966	−1.93992

Table 10
Comparison of the models

		ANFIS	Neural network	Multiple regression
Learning algorithm		Hybrid	Back-propagation	Stepwise regression
Standard deviation	Thermally developing	0.9917003	1.007945	1.756972
	Simultaneously developing	1.009565	1.010707	1.727440
Training error	Thermally developing	0.0035014	0.134140	–
	Simultaneously developing	0.00875	0.209694	–
Test error	Thermally developing	0.03290	0.422487	–
	Simultaneously developing	0.02680	0.238661	–

until none of the remaining variables meet the removal criterion. Variable selection terminates when no more variables meet entry and removal criteria [37]. The results obtained with the multiple linear regression analysis are presented in Tables 8 and 9 for the thermally developing and simultaneously developing flows, respectively. Standard deviations of the thermally developing and simultaneously developing flow were calculated as 1.756972 and 1.727440, respectively. Standard deviations are obtained using the following equation:

$$S = \sqrt{\left(\frac{\sum(\text{Experimental} - \text{Estimated})^2}{n-1}\right)} \tag{21}$$

A multi-layered feed-forward back-propagation algorithm was used in the neural network analysis of the present study. The back-propagation model has three layers of neurons: an input layer, a hidden layer, and an output layer, as shown in Fig. 1. The flow chart of the back-propagation learning algorithm is illustrated in Fig. 2. The algorithm of the training a back-propagation network is explained in detail in the section of introduction. The results obtained with the multi-layered feed-forward back-propagation algorithm are presented in Tables 8 and 9 for the thermally developing and simultaneously developing flows, respectively. Standard deviations were determined to be equal to 1.007945 and 1.010707 for the thermally developing and simultaneously developing flows, respectively.

The comparison of the ANFIS, multiple linear regression, and neural network is presented in Table 10. The comparison shows that:

(i) The maximum standard deviations were obtained with the multiple linear regression,
(ii) the standard deviation of the neural network is higher than that of the ANFIS,
(iii) the training and test errors of the neural network are higher than those of the ANFIS.

Shortly it may be stated that the ANFIS yields the most accurate results.

7. Conclusions

This study was conducted to demonstrate the usefulness of the artificial intelligence techniques for the prediction of transient heat transfer. An adaptive neuro-fuzzy inference system was applied for the transient heat transfer in thermally and simultaneously developing circular duct flow, subjected to a sinusoidally varying inlet temperature. The accuracy of predictions and the adaptability of the ANFIS have been examined. The ANFIS indicated that it was able to learn the training data set and accurately predict the output of unseen test data. The results obtained with the ANFIS are also compared to those of a multiple linear regression and a neural network with a multi-layered feed-forward back-propagation algorithm. The comparison showed that the ANFIS performed better than the multiple linear regressions and the neural network. Although the present study has produced promising preliminary results, to provide an affordable means of capturing transient convective heat transfer data and knowledge in a documented form available for all, this study should be progressed.

References

[1] S. Kakaç, Transient forced convection heat transfer in a channel, Waerme Stoffuebertragung Bd. 1 (1968) 169–176.
[2] R.M. Cotta, M.N. Ozisik, Laminar forced convection inside ducts with periodic variation of inlet temperature, Internat. J. Heat Mass Transfer 10 (1986) 1495–1501.
[3] W. Li, S. Kakaç, Unsteady thermal entrance heat transfer in laminar flow with a periodic variation of inlet temperature, Internat. J. Heat Mass Transfer 34 (1991) 2581–2592.
[4] S. Kakaç, W. Li, R.M. Cotta, Unsteady laminar forced convection in ducts with periodic variation of inlet temperature, J. Heat Transfer 112 (1990) 913–920.
[5] D.M. Brown, Experimental investigation of transient forced convection in a circular duct for timewise variation of inlet temperature, Master Thesis, Dept. of Mech. Eng., University of Miami, 1992.
[6] D.M. Brown, W. Li, S. Kakaç, R. Oskay, Numerical and experimental analysis of unsteady heat transfer with periodic variation of inlet temperature in circular ducts, Internat. Comm. Heat Mass Transfer 20 (1993) 883–899.
[7] H. Kawamura, Experimental and analytic study of transient heat transfer for turbulent flow in a circular tube, Internat. J. Heat Mass Transfer 20 (1977) 443–450.

[8] J.S. Travelho, V.F.N. Santos, Solution for transient conjugated forced convection in the thermal entrance region of a duct with periodically varying inlet temperature, J. Heat Transfer 113 (1992) 558–562.
[9] S.C. Chen, N.R. Anand, D.R. Tree, Analysis of transient laminar convective heat transfer inside a circular duct, J. Heat Transfer 105 (1983) 922–924.
[10] S. Kakaç, Y. Yener, Exact solution of the transient forced convection energy equation for time wise variation of inlet temperature, Internat. J. Heat Mass Transfer 26 (1972) 2205–2214.
[11] O. Comakli, N. Sozbir, D.M. Brown, S. Kakaç, C.A.C. Santos, Transient heat transfer in thermally and simultaneously developing circular duct flow, in: 9th International Conference on Thermal Engineering and Thermogrammetry, 14–16 June, Budapest, Hungary, 1995, pp. 58–63.
[12] J. Sucec, A.M. Sawant, Unsteady, conjugated, forced convection heat transfer in a parallel plate duct, Internat. J. Heat Mass Transfer 27 (1984) 95–101.
[13] M. Coban, Numerical investigation of unsteady forced convection in a duct, Ph. Thesis, Sakarya University, 2001.
[14] I. Ekmekci, M. Coban, A. Kurt, N. Sozbir, S. Ozcelebi, Investigation of forced convection in a duct with artificial neural network, in: 3rd Int. Symp. on Intelligent Manufacturing Systems, Sakarya University, Sakarya, Turkey, 2001, pp. 30–31.
[15] S.A. Kalogirou, Applications of artificial neural-networks for energy systems, Appl. Energy 67 (2000) 17–35.
[16] K. Xu, A.R. Luxmoore, L.M. Jones, F. Deravi, Integration of neural networks and expert systems for microscopic wear particle analysis, Knowledge-Based Systems 11 (1998) 213–227.
[17] L.A. Zadeh, Fuzzy sets, Information Control 8 (1965) 338–353.
[18] J. Jang, ANFIS: Adaptive network-based fuzzy inference systems, IEEE Trans. Systems Man Cybernet. 23 (1993) 665–685.
[19] J. Thibault, B.P.A. Grandjean, A neural network methodology for heat transfer data analysis, Internat. J. Heat Mass Transfer 34 (1991) 2063–2070.
[20] K. Jambunathan, S.L. Hartle, S. Ashforth-Frost, V.N. Fontama, Evaluating convective heat transfer coefficients using neural networks, Internat. J. Heat Mass Transfer 39 (1996) 2329–2332.
[21] G. Diaz, Sen Mihir, K.T. Yang, R.L. McClain, Dynamic prediction and control of heat exchangers using artificial neural networks, Internat. J. Heat Mass Transfer 44 (2001) 1671–1679.
[22] S. Bittati, L. Piroddi, Nonlinear Identification and Control of a heat exchanger: A neural network approach, J. Franklin İnst. B 334 (1997) 135–153.
[23] G. Scalabrin, L. Piazza, Analysis of forced convection heat transfer to supercritical carbon dioxide inside tubes using neural networks, Internat. J. Heat Mass Transfer 46 (2003) 1139–1154.
[24] D.F. Cook, C.T. Ragsdale, R.L. Major, Combining a neural network with a genetic algorithm for process parameter optimization, Engrg. Appl. Artificial Intelligence 13 (2000) 391–396.
[25] N. Sözbir, Experimental Investigation of Unsteady Forced Convection in a Rectangular Channel with or without Arrays of Block-Like Electronic Component, Report, University of Miami, Coral Gables, Florida, 1995.
[26] T. Takagi, M. Sugeno, Fuzzy identification of systems and its applications to modeling and control, IEEE Trans. Syst. Man Cybernet. 15 (1985) 116–132.
[27] E.H. Mamdani, S. Assilian, An experiment in linquistic synthesis with a fuzzy logic controller, Internat. J. Man-Mach. Stud. 7 (1975) 1–13.
[28] M. Sugeno, Industrial Applications of Fuzzy Control, Elsevier, Amsterdam, 1985.
[29] Y. Tsukamoto, An approach to fuzzy reasoning method, in: M.M. Gupta, R.K. Ragade, R.R. Yager (Eds.), Advances in Fuzzy Set Theory and Applications, North-Holland, Amsterdam, 1979, pp. 137–149.
[30] J.S.R. Jang, C.T. Sun, E. Mizutani, Neuro-Fuzzy and Soft Computing: A Computational Approach to Learning and Machine Intelligence, Prentice Hall International, London, 1997.
[31] H. Takagi, I. Hayashi, Artificial neural network driven fuzzy reasoning, Internat. J. Approx. Reasoning 5 (1991) 191–212.
[32] F.A. Alturki, A. Abdennour, Design and simplification of adaptive Neuro-Fuzzy inference controllers for power plants, Electrical Power & Energy Systems 21 (1999) 465–474.
[33] A. Sfetsos, A comparison of various forecasting techniques applied to mean hourly wind speed time series, Renewable Energy 21 (2000) 23–35.
[34] M.J. Norusis, SPSS Base System User's Guide, SPSS Inc, Chicago, 1990.
[35] P. Newbold, Statistics for Business and Economics, Prentice-Hall, Englewood Cliffs, NJ, 1988.
[36] N.R. Draper, H. Smith, Applied Regression Analysis, Wiley, New York, 1981.
[37] M.D. Kaya, A.S. Hasiloglu, M. Bayramoglu, H. Yesilyurt, F. Ozok, A new approach to estimate anthropometric measurements by adaptive neuro-fuzzy inference system, Internat. J. Indust. Ergonom. 32 (2003) 105–114.